

Study of $V_L V_L \rightarrow \bar{t} t$ at the ILC Including NLO QCD Corrections

Stephen Godfrey^a and Shou-hua Zhu^{a,b}

^aOttawa-Carleton Institute for Physics, Department of Physics,
Carleton University, Ottawa, Canada K1S 5B6

^bInstitute of Theoretical Physics, School of Physics,
Peking University, Beijing 100871, China

(Dated: February 8, 2020)

In the event that the Higgs mass is large or that the electroweak interactions are strongly interacting at high energy, top quark couplings to longitudinal components of the weak gauge bosons could offer important clues to the underlying dynamics. It has been suggested that precision measurements of $W_L W_L \rightarrow \bar{t} t$ and $Z_L Z_L \rightarrow \bar{t} t$ might provide hints of new physics. In this paper we present results of QCD corrections to $V_L V_L \rightarrow \bar{t} t$ scattering at the ILC. We find that corrections to cross sections can be as large as 30% and must be accounted for in any precision measurement of $V V \rightarrow \bar{t} t$.

PACS numbers: 12.38.Bx, 14.65.Ha, 12.60.-i, 14.80.Bn

I. INTRODUCTION

Understanding the mechanism of electroweak symmetry breaking (EWSB) is a primary goal of the Large Hadron Collider (LHC) [1]. Numerous possibilities have been proposed and in some cases their experimental signatures have been studied in detail [2]. The models can be roughly divided into two scenarios. The first possibility is a weakly interacting weak sector which implies light Higgs bosons and naturally leads to Supersymmetry which predicts many new supersymmetric particles [3]. The alternative scenario is a strongly interacting Higgs sector (SIWS) [4] most often described by dynamical symmetry breaking [5]. Recently, additional new approaches to EWSB have emerged, such as the Little Higgs model [6, 7, 8, 9, 10, 11] which contain ingredients from both scenarios and other alternative approaches such as "Higgsless" models [12, 13, 14]. Although the light Higgs mass scenario is favoured by precision electroweak tests, models with heavy Higgs bosons can be accommodated by the data [15, 16, 17]. It is this latter possibility that we wish to study.

While the signature for the weakly interacting weak sector is the production of light Higgs bosons and possibly additional particles and many of the newer models predict relatively light extra gauge bosons, the signal for a SIWS will almost certainly be more subtle [18]. In the SIWS scenario W -boson interactions can be described by an effective Lagrangian with the coefficients in \mathcal{L}_{eff} constrained by experiment [19]. Detailed studies have been made for the LHC [4, 20, 21, 22].

Because the t -quark mass is the same order of magnitude as the scale of EWSB it has long been suspected that t -quark properties may provide hints about the nature of EWSB [23, 24, 25, 26, 27, 28, 29]. To this end studies have been performed of $V V \rightarrow \bar{t} t$ both in terms of the

sensitivity to M_H [30, 31, 32], and in terms of an effective Lagrangian describing vector boson t -quark interactions [33]. Moreover, this process should be sensitive to models such as top-colour [34] and the top see-saw model [35]. Due to the Goldstone boson equivalence theorem [36] the longitudinal gauge bosons (W_L ; Z_L) are equivalent to the Goldstone modes at energies much larger than their mass so that they reflect the properties of EWSB. In principle, $V_L V_L \rightarrow \bar{t} t$ can be studied at both hadron colliders through $q_1 q_2 \rightarrow q_1^0 q_2^0 V_L V_L^0$ and at high energy $e^+ e^-$ colliders via $e^+ e^- \rightarrow \gamma^* \gamma^* V_L V_L^0$ or $Z^* \rightarrow V_L V_L^0 + X$ [24, 30, 31, 32, 37]. While the LHC will be the highest energy collider to explore the TeV energy region the overwhelming QCD backgrounds for $t\bar{t}$ production will likely make it impossible to study the $V_L V_L \rightarrow \bar{t} t$ subprocess [38].

The ILC offers a much cleaner environment to study the $V_L V_L \rightarrow \bar{t} t$ subprocess. The simplest approach is to study how the $t\bar{t}$ cross section varies with M_H . This has been studied by several authors [30, 31, 32]. The tree-level Feynman diagrams for the SM process are given in Fig. 1. The $e^+ e^- \rightarrow \bar{t} t$ cross section is shown as a function of M_H in Fig. 2 for an $e^+ e^-$ collider with centre of mass energy $\sqrt{s_{e^+ e^-}} = 1 \text{ TeV}$. We convoluted the effective W approximation (EWA) distributions [39, 40] with the $W_L^+ W_L^- \rightarrow \bar{t} t$ cross section to obtain the $e^+ e^- \rightarrow \bar{t} t$ cross sections and included the kinematic cuts $M_{t\bar{t}} > 400 \text{ GeV}$ and $p_T^{t\bar{t}} > 10 \text{ GeV}$. The values for these kinematic cuts were chosen so that in the former case the EWA is reasonably reliable and in the latter case to reduce various backgrounds. This is discussed more fully in section IV.

A more general approach is to parameterize interactions in a nonlinearly realized electroweak chiral Lagrangian [19] which is appropriate if the EWSB dynamics is strong with no Higgs bosons at low energies. For illustrative purposes we show the sensitivity of the cross sections to a representative dimension five operator;

$$\mathcal{L}_1^{eff} = \frac{a_1}{\Lambda} t\bar{t} W^+ W^- \quad (1)$$

where the coefficient a_1 is naively expected to be of order 1 when the cut-off of the theory is taken to be $\Lambda = 4v = 3.1 \text{ TeV}$ with $v = 246 \text{ GeV}$, the vacuum expectation value of the SM Higgs field. We do not rigorously follow the chiral Lagrangian approach and simply include the operator of Eqn. 1 as an additional $WWtt$ interaction. The effect of varying a_1 for an e^+e^- collider with $\sqrt{s_{e^+e^-}} = 1 \text{ TeV}$ is shown in Fig. 3 using the EWA and the same kinematic cuts as before. ($e^+e^- \rightarrow tt$) is shown for $M_H = 120, 500,$ and 1000 GeV and for $M_H = 1$. The latter case is referred to in the literature as the "low energy theorem" (LET) model. A careful analysis by Ref. [33, 41] finds that the $V_L V_L tt$ coupling can be measured to an accuracy of ~ 0.1 at 95% C.L. (with the cut-off scale of $\Lambda = 3.1 \text{ TeV}$ divided out as expressed in Eqn. 1).

These approaches are complementary to studies based on specific models and on the linear realization of EW symmetry breaking which includes physical Higgs bosons in the particle spectrum. The crucial point is that precision measurements of top-quark interactions could play an important role in understanding the mechanism of EW SB. But to be able to attach meaning to precision measurements it is necessary to understand radiative corrections, both electroweak and QCD.

In this paper we quantify the importance of QCD radiative corrections for the process $V_L V_L \rightarrow tt$. We focus on the leading order QCD corrections to the tree level electroweak $V_L V_L \rightarrow tt$ process in the SM at the ILC. We begin in section II by summarizing the effective W approximation and how it is implemented in our calculations. The bulk of the section is devoted to how we calculated the QCD corrections. Numerical results are given in section III with section IV devoted to a discussion of other aspects which should be considered in a complete calculation of tt production. Concluding comments are given in the final section.

II. CALCULATIONS

We are interested in the subprocesses $VV \rightarrow tt$ which occur in the processes

$$e^+e^- \rightarrow \gamma^* Z + VV \rightarrow \gamma^* Z + tt \quad (2)$$

where $\gamma^* Z$ is for the $W^+W^- \rightarrow tt$ subprocess and e^+e^- for the $ZZ \rightarrow tt$ subprocess. Before proceeding to

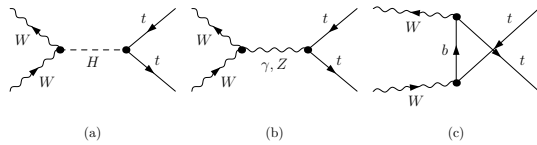


FIG. 1: The tree level diagrams for $W^+W^- \rightarrow tt$.

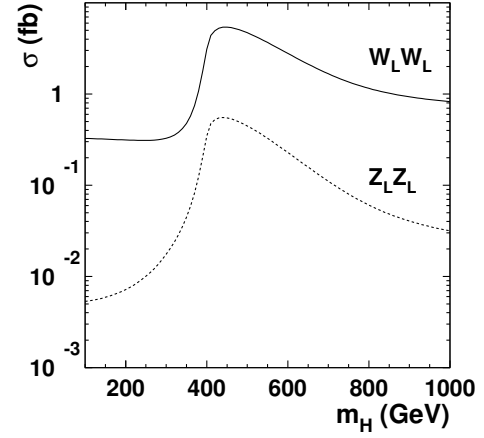


FIG. 2: The solid line is for $(e^+e^- \rightarrow tt)$ (the $W_L^+W_L^- \rightarrow tt$ subprocess) and the dotted line is for $(e^+e^- \rightarrow e^+e^- tt)$ (the $Z_L Z_L \rightarrow tt$ subprocess) as a function of M_H for an e^+e^- collider with centre of mass energy $\sqrt{s_{e^+e^-}} = 1 \text{ TeV}$ and kinematic cuts $m_{tt} > 400 \text{ GeV}$ and $p_T^{tt} > 10 \text{ GeV}$.

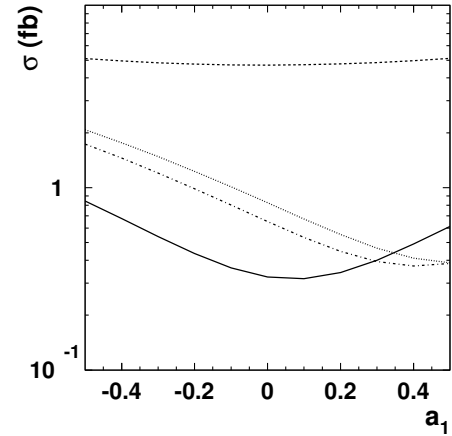


FIG. 3: $(e^+e^- \rightarrow tt)$ (the $W_L^+W_L^- \rightarrow tt$ subprocess) vs the $WWtt$ coupling a_1 for $\sqrt{s_{e^+e^-}} = 1 \text{ TeV}$ with the same kinematic cuts as Fig. 2. The solid line is for $M_H = 120 \text{ GeV}$, the dashed line for $M_H = 500 \text{ GeV}$, the dotted line for $M_H = 1000 \text{ GeV}$, and the dot-dashed line for $M_H = 1$ (the LET scenario).

the QCD corrections we briefly summarize the effective vector boson approximation (EVA).

A. The Effective Vector Boson Approximation

In the effective vector boson approximation the W and Z bosons are treated as partons inside the electron

[39, 40]. The total cross section is then obtained by integrating the W (of Z) luminosities with the subprocess cross section [37].

$$\sigma(e^+e^- \rightarrow V_1 V_2 \rightarrow tt) = \sum_{V_1, V_2} \int_{s_{\text{min}}}^s \frac{dL}{d^2} \hat{\sigma}(V_1 V_2 \rightarrow tt) \quad (3)$$

where V_1 and V_2 are the V 's polarization, $\frac{dL}{d^2} = \frac{d^3x}{s} \delta(s - 2x)$ with s and x the e^+e^- and $V_1 V_2$ centre-of-mass energy respectively, and L is the $V_1 V_2$ luminosity given by

$$\frac{dL}{d^2} = \int \frac{dx}{x} f_{V_1=e}(x) f_{V_2=e}(s/x) \quad (4)$$

The $f_{V=e}$ distributions are given by [39, 40]

$$f_{V=e}(x) = \frac{C}{16^2 x} \left[(g_V^f - g_A^f)^2 + (g_V^f + g_A^f)^2 (1-x)^2 \right] \log \frac{4E^2}{M_V^2} \quad (5)$$

$$f_{VL=e}(x) = C \frac{(g_V^f)^2 + (g_A^f)^2}{4^2} \frac{1-x}{x} \quad (6)$$

for the transverse and longitudinal V 's respectively and where for a W boson $C = g^2=8$, $g_V = g_A = 1$ and for a Z boson $C = g^2=\cos^2 \theta_w$, $g_V = \frac{1}{2}T_3 - Q \sin^2 \theta_w$, $g_A = \frac{1}{2}T_3$ with g the coupling constant for the weak-isospin group $SU(2)_L$ and E the energy of the initial lepton. With these expressions for the V distributions, the luminosity for LL scattering simplifies to [39, 40]:

$$\frac{dL_{LL}}{d^2} = \frac{[(g_V^e)^2 + (g_A^e)^2]^2}{16^4} [2(1-x)(1+x) \log \dots] \quad (7)$$

B. $O(\alpha_s)$ corrections to $VV \rightarrow tt$

We next describe how we calculated the $O(\alpha_s)$ corrections for the process $W^+W^- \rightarrow tt$. The results for $ZZ \rightarrow tt$ are obtained the same way. To obtain our results we used the FeynArts, FormCalc and LoopTools packages [42]. We point out details specific to our calculation but refer the interested reader to the descriptions of the packages for further information.

The tree-level Feynman diagrams for $W^+W^- \rightarrow tt$ are given in Fig. 1 and the virtual diagrams are shown in Fig. 4a. The infrared singularity in the vertex corrections are cancelled by the soft contributions from the process $W^+W^- \rightarrow ttg$ which are shown in Fig. 4b. Since only soft photon formulas are embedded in the FeynArts/FormCalc/LoopTools packages, to accommodate the soft gluons we modified the corresponding formulas with the substitution $eQ \rightarrow g_s T_a$. For processes with no triple gluon vertex present, introducing a gluon mass is equivalent to standard dimensional regularization. Introducing a small finite gluon mass is easily included using the packages we employ, so for convenience we regulate the

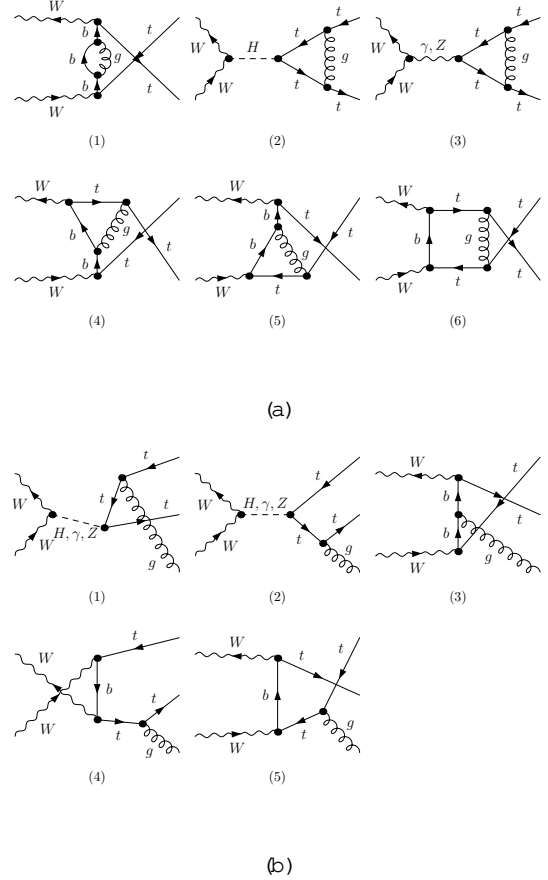


FIG. 4: QCD corrections to $W^+W^- \rightarrow tt$. (a) Virtual QCD contributions to $W^+W^- \rightarrow tt$. (b) Feynman diagrams for $W^+W^- \rightarrow tt+g$.

IR-singularity this way. This approach has the additional benefit that varying the value of the gluon mass acts as a check of the numerical cancellations between the different contributions.

The cross-sections are calculated by replacing the Born matrix element squared by

$$|\mathcal{M}_{\text{Born}}|^2 \rightarrow |\mathcal{M}_{\text{Born}}|^2 (1 + \text{soft}) + 2\text{Re}(\mathcal{M}_{\text{Born}} \mathcal{M}) \quad (8)$$

where \mathcal{M} is the sum of the one-loop Feynman diagrams and the corresponding counter-term diagrams and soft is the soft-gluon correction factor coming from the $2 \rightarrow 3$ process. The hard contribution from the $2 \rightarrow 3$ process is also $O(\alpha_s)$ and will be discussed further below. Thus, Eqn. 8 yields the cross-section including all $O(\alpha_s)$ corrections but neglects the $O(\alpha_s^2)$ corrections that are included in the dropped $|\mathcal{M}|^2$ contribution.

To deal with renormalization associated with the ultraviolet divergences we adopt the on-shell renormalization scheme and use dimensional regularization. In the on-shell renormalization scheme for the external quark legs, the top-quark self-energy is cancelled by its corresponding counter-term. For this reason we do not explicitly show the top-quark self energy diagrams in Fig. 4. The scale dependence in this calculation only

enters in \hat{s} and we take it to be \hat{s} . We will discuss uncertainties due to this choice below.

To estimate uncertainties due to scale dependence we vary the scale by factor of two smaller and a factor of two larger at the peak in the subprocess, \hat{s} , which is the dominant contribution to the e^+e^- cross sections. We find an uncertainty of 15% in \hat{s} which leads to at most 4% uncertainty in the K-factor.

The software packages we used handle renormalization by employing numerical factors. For example, the UV divergence is represented by a numerical factor ϵ . Because our results must be independent of these factors we can vary them to check the consistency of our results. In particular, the UV finiteness is checked by verifying the independence of the results to ϵ and in the on-mass shell renormalization scheme to the dimensional regularization scale parameter μ .

As mentioned above, the IR singularity was regulated by introducing a finite gluon mass which is allowed when no triple-gluon vertex contributes to the amplitude. The cancellation of the finite gluon contributions from the vertex correction with the soft gluon production in $W^+W^- \rightarrow tt\bar{t}\bar{t}$ is a strong test of the veracity of our results. We performed this check and also verified that the results are independent of the gluon regulator mass but for the sake of brevity do not show plots of these results.

A final check is to verify that the results are independent of the soft cutoff energy of the emitted gluon which divides the cross section into a piece with a soft gluon emitted and a piece with a hard gluon emitted. To do so we sum the results of the hard $W^+W^- \rightarrow tt\bar{t}\bar{t}$ process with the soft $W^+W^- \rightarrow tt\bar{t}\bar{t}$ plus 1-loop results. While individually the hard and soft pieces are dependent on the soft cutoff energy of the emitted gluon, the sum will not be. We have checked that our results are indeed independent of the gluon cutoff energy.

To obtain cross sections from the analytical results for the squared amplitudes, the FormCalc package integrates phase space using gaussian quadrature for the 2 to 2 process and the VEGAS Monte Carlo integration package for the 2 to 3 process.

III. RESULTS

In Fig. 5 we show the tree level electroweak and leading order QCD corrected cross sections for the subprocesses $W^+W^- \rightarrow tt\bar{t}\bar{t}$ and $ZZ \rightarrow tt\bar{t}\bar{t}$ for a Higgs boson mass of 500 GeV and for all W and Z polarizations. In all cases we include the $tt + g$ final state in the NLO results. To separate out the hard gluon case depends on details of the detector and the $j\bar{t}$ finding algorithms which is beyond the scope of this paper. As before, we include in these and all subsequent results the kinematic cuts $m_{tt} > 400$ GeV and $p_T^{t\bar{t}} > 10$ GeV. The Born results agree with previous results [30]. The longitudinal scattering cross section is much larger than the TT and TL cases. Since it is the longitudinal gauge boson processes which corresponds to

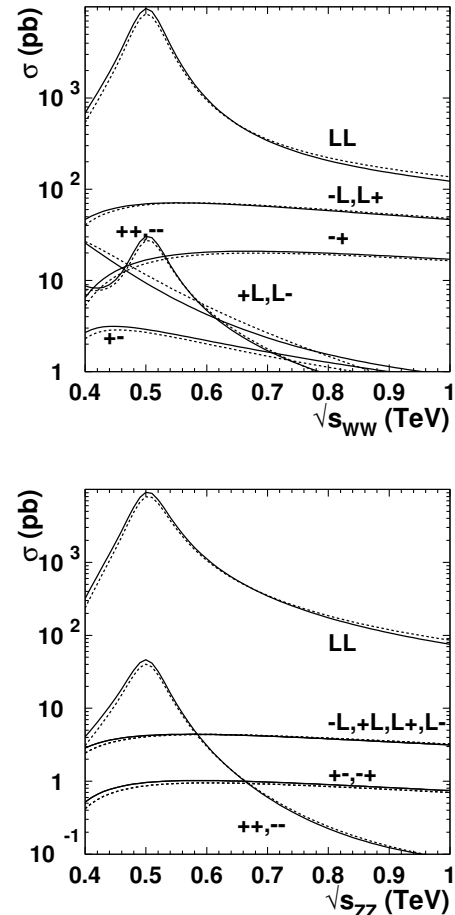


FIG. 5: Cross sections as a function of $\sqrt{\hat{s}}$ for the subprocesses (a) $W^+W^- \rightarrow tt$ and (b) $ZZ \rightarrow tt$. In both cases $m_H = 500$ GeV at LO QCD corrected (solid) and electroweak tree level (dashed).

the Goldstone bosons of the theory we will henceforth only include results for $V_L V_L$ scattering. In Fig. 6 we show the cross section only including longitudinal W and Z scattering as a function of the e^+e^- centre of mass energy for several representative Higgs masses including the $M_H = 1$ case (corresponding to the LET).

The QCD corrections to longitudinal scattering are often presented as a K-factor, normally defined as the ratio of the NLO to LO cross sections. Because the QCD corrections we have calculated in this paper are LO corrections to a tree level electroweak result we are taking the K-factor factor to be the ratio of the cross section with the LO QCD corrections and the tree level electroweak cross sections. The K-factors for $(e^+e^- \rightarrow tt)$ which goes via $W_L^+ W_L^-$ fusion and for $(e^+e^- \rightarrow e^+e^- tt)$ which goes via $Z_L Z_L$ fusion are shown in Fig. 7 as a function of the e^+e^- centre of mass energy. K-factors are shown for $M_H = 120$ GeV, 500 GeV, 1 TeV, and the LET case (using the same kinematic cuts as before). The QCD corrections are largest for $M_H = 500$ GeV with

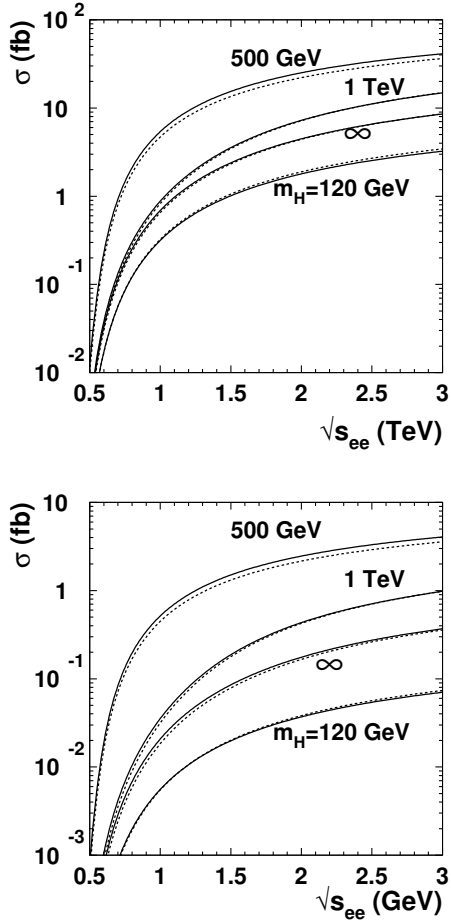


FIG. 6: Cross sections as a function of $\sqrt{s_{e^+e^-}}$ for (a) $e^+e^- \rightarrow t\bar{t}$ via $W_L^+W_L$ fusion and for (b) $e^+e^- \rightarrow t\bar{t}$ via $Z_L Z_L$ fusion. In both cases the solid line is the LO QCD corrected cross section and the dashed line is the electroweak tree level cross section.

K-factors ranging from over 1.2 for $\sqrt{s_{e^+e^-}} = 500$ GeV to 1.15 for $\sqrt{s_{e^+e^-}} = 1$ TeV. The corrections decrease as the e^+e^- centre-of-mass energy increases. The corrections are smallest for a light Higgs but in that case we will probably study top-Higgs couplings in other processes such as associated top-Higgs production. As can be seen from Fig. 7 the $M_H = 1$ TeV and LET cases lie between these two extremes. The variation of the K-factor with M_H is shown more explicitly in Fig. 8. The fact that the K-factor is largest for $M_H = 500$ GeV in Fig. 7 and that it peaks at $M_H \approx 400$ GeV in Fig. 8 is a threshold effect which is an artifact of the kinematic cut we imposed on the $t\bar{t}$ invariant mass. When we pass through the kinematic threshold the dominant contribution to the $t\bar{t}$ threshold comes from the s-channel Higgs resonance. This threshold behavior is also seen in Fig. 3 of Ref. [30] but at a different value of M_H reflecting the different $M_{t\bar{t}}^{\text{cut}}$ used in that paper. This threshold region also corresponds to a region of low Q^2 relevant to soft

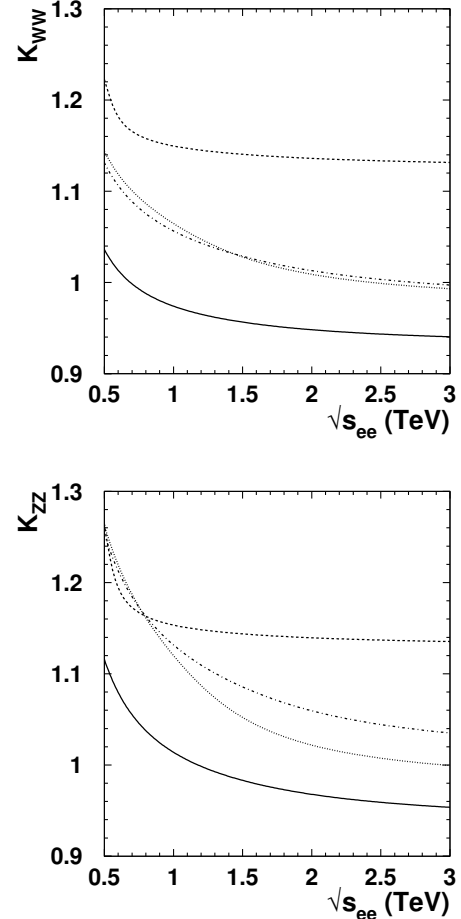


FIG. 7: The K-factors as a function of $\sqrt{s_{e^+e^-}}$ for (a) $e^+e^- \rightarrow t\bar{t}$ (via $W_L^+W_L$ fusion) and for (b) $e^+e^- \rightarrow t\bar{t}$ (via $Z_L Z_L$ fusion). In both cases the solid line is for $M_H = 120$ GeV, the dashed line for $M_H = 500$ GeV, the dotted line for $M_H = 1$ TeV, and the dot-dashed line for $M_H = 1$ (LET). See text for an explanation of the K-factor.

gluon emission resulting in larger QCD corrections. As the phase space opens up the QCD corrections are expected to decrease which is what is observed. One also sees in Fig. 8 how the K-factor decreases as $\sqrt{s_{e^+e^-}}$ increases. The important point one comes away with from Fig. 7 and 8 is that it is clear that QCD corrections are not insignificant compared to the effects we might wish to study such as top Yukawa couplings or anomalous VVtt couplings.

A brief comment about uncertainties due to scale dependence is in order. As stated above, the scale dependence in this calculation only enters in μ_s which we took to be \hat{s} . To estimate uncertainties due to scale dependence we vary the scale by a factor of two smaller and a factor of two larger at the peak in the subprocess, \hat{s} , which is the dominant contribution to the e^+e^- cross sections. We find an uncertainty of 15% in μ_s which leads to at most 4% uncertainty in the K-factor.

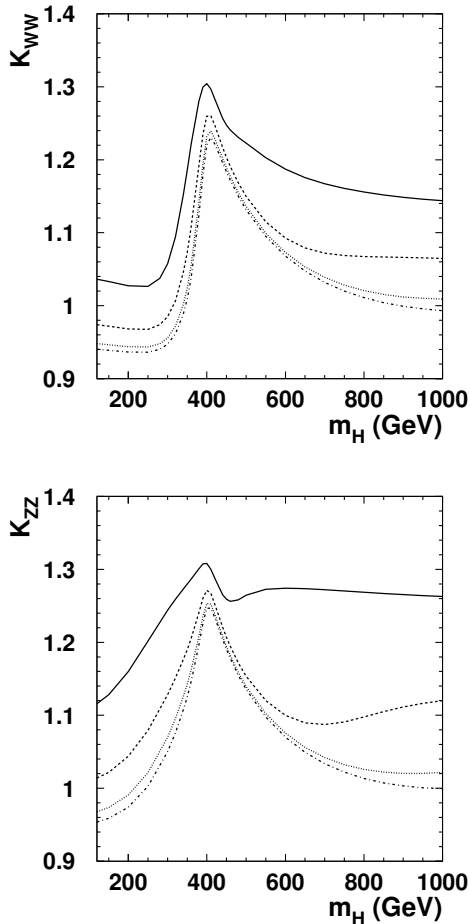


FIG. 8: The K -factor as a function of M_H for (a) $e^+e^- \rightarrow \tau^+\tau^-$ (via $W_L^+W_L^-$ fusion) and for (b) $e^+e^- \rightarrow e^+e^-\tau^+\tau^-$ (via $Z_L Z_L$ fusion). In both cases the solid line is for $\sqrt{s_{e^+e^-}} = 500$ GeV, the dashed line for $\sqrt{s_{e^+e^-}} = 1$ TeV, the dotted line for $\sqrt{s_{e^+e^-}} = 2$ TeV, and the dot-dashed line for $\sqrt{s_{e^+e^-}} = 3$ TeV. See text for an explanation of the K -factor.

IV. DISCUSSION

In this paper we concentrated on QCD corrections. There are equally important considerations and contributions that we have neglected. For completeness we briefly describe them here.

Backgrounds are always an important ingredient and have been discussed in Ref. [4, 28, 32]. Briefly, the relevant signal is a $t\bar{t}$ pair with missing transverse momentum carried by the neutrinos or from the beam electrons not observed by the detector. The largest background is direct $t\bar{t}$ production. It can be suppressed by requiring missing mass greater than some minimum value. This background can be further reduced by choosing the jet association that best reconstructs the t and W masses. Another significant background is $t\bar{t}$ production via other gauge boson fusion with the largest being $\gamma\gamma \rightarrow t\bar{t}$ [37]. This can be reduced by requiring the missing transverse

energy to be greater than some value, with a value of 50 GeV used by Akaraz and Morales for a TeV collider [32]. The main background we mention is $e^+e^- \rightarrow \gamma t\bar{t}$ where the photon escapes the detector but is sufficiently hard to generate the required p_T . Most of this background can be eliminated with an appropriate cut on the p_T^{tt} of the $t\bar{t}$ pair [41]. Additionally the signal could be enhanced using polarized beams [41].

At present the electroweak radiative corrections for top quark production have not been calculated and there are ambiguities which still need to be better understood. In general, when the Higgs boson mass is heavy, the electroweak correction to the process contains the enhancement factor m_H^2/M_W^2 which will be significant. However, S -matrix elements of $VV \rightarrow t\bar{t}$ are not well-defined for unstable external particles so are problematic for higher-order calculations that include the Higgs width at the Born level. The discussion of this issue has been given for the process $W^+W^- \rightarrow W^+W^-$ in [43]. The full process with stable initial and final particles needs to be considered if one includes electroweak corrections consistently. This is beyond the scope of this paper.

The accuracy of the effective W approximation has been studied by a number of authors. Assuming a cut on the invariant mass of $M_{t\bar{t}} > 500$ GeV the resulting cross sections typically agree to about 10% with the exact calculation [41]. This is the same order of magnitude as the effects we are interested in measuring and the QCD corrections considered in this paper. Therefore, an exact calculation would be required for precision measurements of $t\bar{t}$ cross sections.

Finally, we mention that the subprocess $W^+W^- \rightarrow t\bar{t}$ is also possible in $\gamma\gamma$ collisions but the standard model direct processes overwhelm this subprocess by several orders of magnitude. Analogous to the e^+e^- case one can use the effective W luminosity inside photons [44, 45]. It is possible that judicious choices of kinematic cuts could enhance the signal; in $\gamma\gamma \rightarrow t\bar{t}$ the cross section is dominated by the top-quarks collinear to the beam while in the W -fusion process the spectator W 's along the beam direction could be used to tag events [44]. We leave this process for a future study.

V. CONCLUSIONS

In the event that the Higgs mass is heavy and the electroweak sector is strongly interacting it is quite possible that the underlying theory will manifest itself in the interactions between the top quark and longitudinal component of gauge bosons. Different aspects of this have been studied but the common theme is that precision measurements at a future high energy e^+e^- would be necessary to understand the underlying dynamics. In this paper we studied the LO QCD corrections to the tree level electroweak process $VV \rightarrow t\bar{t}$. We found that they can be quite substantial, the same size as the effects we wish to study, so that they need to be taken

into account when studying tt production. Although the kinematic cuts that are chosen will change the numerical results slightly, the LO QCD corrections are understood and should not pose a barrier in studying these processes.

Acknowledgments

SG thanks Frank Petriello for helpful discussions. This research was supported in part by the Natural Sciences

and Engineering Research Council of Canada. SZ was also supported in part by the Natural Science Foundation of China under grant no. 90403004

-
- [1] For a recent review see R. Barbieri, Lectures given at Cargèse School of Particle Physics and Cosmology: the Interface, Cargèse, Corsica, France, 4-16 Aug 2003. [arXiv:hep-ph/0312253](#).
- [2] ATLAS detector and physics performance. Technical design report. Vol. 2, CERN-LHCC-99-15
- [3] H. Baer et al., [arXiv:hep-ph/9503479](#).
- [4] T. L. Barklow et al., eConf C960625, STC118 (1996) [[arXiv:hep-ph/9704217](#)].
- [5] C. T. Hill and E. H. Simmons, Phys. Rept. 381, 235 (2003) [Erratum-ibid. 390, 553 (2004)] [[arXiv:hep-ph/0203079](#)].
- [6] N. Arkan-Hamed, A. G. Cohen and H. Georgi, Phys. Lett. B 513, 232 (2001) [[arXiv:hep-ph/0105239](#)]; N. Arkan-Hamed, A. G. Cohen, T. Gregoire and J. G. Wacker, JHEP 0208, 020 (2002) [[arXiv:hep-ph/0202089](#)]; N. Arkan-Hamed, A. G. Cohen, E. Katz, A. E. Nelson, T. Gregoire and J. G. Wacker, JHEP 0208, 021 (2002) [[arXiv:hep-ph/0206020](#)]; N. Arkan-Hamed, A. G. Cohen, E. Katz and A. E. Nelson, JHEP 0207, 034 (2002) [[arXiv:hep-ph/0206021](#)].
- [7] I. Low, W. Skiba and D. Smith, Phys. Rev. D 66, 072001 (2002) [[arXiv:hep-ph/0207243](#)].
- [8] For a recent review see M. Schmaltz, Nucl. Phys. Proc. Suppl. 117, 40 (2003) [[arXiv:hep-ph/0210415](#)].
- [9] T. Han, H. E. Logan, B. McElrath and L. T. Wang, Phys. Rev. D 67, 095004 (2003) [[arXiv:hep-ph/0301040](#)].
- [10] J. L. Hewett, F. J. Petriello and T. G. Rizzo, JHEP 0310, 062 (2003) [[arXiv:hep-ph/0211218](#)].
- [11] M. P. Perelstein, M. E. Peskin and A. Pierce, Phys. Rev. D 69, 075002 (2004) [[arXiv:hep-ph/0310039](#)].
- [12] C. Csaki, C. Grojean, H. Murayama, L. Pilo and J. Teming, Phys. Rev. D 69, 055006 (2004) [[arXiv:hep-ph/0305237](#)].
- [13] C. Csaki, C. Grojean, L. Pilo and J. Teming, Phys. Rev. Lett. 92, 101802 (2004) [[arXiv:hep-ph/0308038](#)].
- [14] H. Davoudiasl, J. L. Hewett, B. Lillie and T. G. Rizzo, Phys. Rev. D 70, 015006 (2004) [[arXiv:hep-ph/0312193](#)].
- [15] M. E. Peskin and J. D. Wells, Phys. Rev. D 64, 093003 (2001) [[arXiv:hep-ph/0101342](#)].
- [16] M. S. Chanowitz, Phys. Rev. D 66, 073002 (2002) [[arXiv:hep-ph/0207123](#)].
- [17] R. Barbieri, A. Pomarol, R. Rattazzi and A. Strumia, Nucl. Phys. B 703, 127 (2004) [[arXiv:hep-ph/0405040](#)].
- [18] A recent account of these topics is given in LHC/LC Study Group, Physics interplay of the LHC and the ILC, [[hep-ph/0410364](#)].
- [19] S. Dawson and G. Valencia, Nucl. Phys. B 352, 27 (1991); A. Dobado, M. J. Herrero and J. Terron, Z. Phys. C 50, 205 (1991).
- [20] M. S. Chanowitz, [arXiv:hep-ph/9812215](#).
- [21] R. Rosenfeld and J. L. Rosner, Phys. Rev. D 38, 1530 (1988).
- [22] J. Bagger et al., Phys. Rev. D 49, 1246 (1994) [[arXiv:hep-ph/9306256](#)]; J. Bagger et al., Phys. Rev. D 52, 3878 (1995) [[arXiv:hep-ph/9504426](#)].
- [23] M. S. Chanowitz, M. A. Fumman and I. Hinchliffe, Nucl. Phys. B 153, 402 (1979).
- [24] F. Larios and C. P. Yuan, Phys. Rev. D 55, 7218 (1997) [[arXiv:hep-ph/9606397](#)].
- [25] X. Zhang, S. K. Lee, K. Whisnant and B. L. Young, Phys. Rev. D 50, 7042 (1994) [[arXiv:hep-ph/9407259](#)].
- [26] K. Whisnant, B. L. Young and X. Zhang, Phys. Rev. D 52, 3115 (1995) [[arXiv:hep-ph/9410369](#)].
- [27] J. Wudka, [arXiv:hep-ph/9706434](#).
- [28] T. Han, Y. J. Kim, A. Likhoded and G. Valencia, Nucl. Phys. B 593, 415 (2001) [[arXiv:hep-ph/0005306](#)].
- [29] T. Han, G. Valencia and Y. Wang, Phys. Rev. D 70, 034002 (2004) [[arXiv:hep-ph/0405055](#)].
- [30] M. Gintner and S. G. Odfrey, [arXiv:hep-ph/9612342](#);
- [31] E. Ruiz Morales and M. E. Peskin, [arXiv:hep-ph/9909383](#).
- [32] J. Alcaraz and E. Ruiz Morales, Phys. Rev. Lett. 86, 3726 (2001) [[arXiv:hep-ph/0012109](#)].
- [33] F. Larios, T. M. P. Tait and C. P. Yuan, [arXiv:hep-ph/0101253](#).
- [34] C. T. Hill, Phys. Lett. B 266, 419 (1991). See also ref. [5] for a recent review.
- [35] B. A. Dobrescu and C. T. Hill, Phys. Rev. Lett. 81, 2634 (1998) [[arXiv:hep-ph/9712319](#)]; R. S. Chivukula, B. A. Dobrescu, H. Georgi and C. T. Hill, Phys. Rev. D 59, 075003 (1999) [[arXiv:hep-ph/9809470](#)].
- [36] B. W. Lee, C. Quigg and H. B. Thacker, Phys. Rev. D 16, 1519 (1977); M. S. Chanowitz and M. K. Gaillard, Nucl. Phys. B 261, 379 (1985); Y. P. Yao and C. P. Yuan, Phys. Rev. D 38, 2237 (1988); J. Bagger and C. Schmidt, Phys. Rev. D 41, 264 (1990); H. G. J. Velthuis, Phys. Rev. D 41, 2294 (1990); H. J. He, Y. P. Kuang and X. Y. Li, Phys. Rev. Lett. 69, 2619 (1992); H. J. He and W. B. Kilgore, Phys. Rev. D 55, 1515 (1997) [[arXiv:hep-ph/9609326](#)].
- [37] R. P. Kamman, Phys. Rev. D 41, 3343 (1990).
- [38] T. Han, D. L. Rainwater and G. Valencia, Phys. Rev. D 68, 015003 (2003) [[arXiv:hep-ph/0301039](#)].
- [39] R. Cahn and S. Dawson, Phys. Lett. 136B, 196 (1984); (E) Phys. Lett. 138B, 464 (1984); S. Dawson, Nucl.

- Phys. B 249, 42 (1985); M. Chanowitz and M. Gaillard, Phys. Lett. 142B, 85 (1984); G. Kane, W. Repko, and W. Rolnick, Phys. Lett. 148B, 367 (1984); J. Lindfors, Z. Phys. C 28, 427 (1985).
- [40] S. Dawson and S. S. D. Wilkenbrock, Nucl. Phys. B 284, 449 (1987).
- [41] F. Larios, T. Tait and C. P. Yuan, Phys. Rev. D 57, 3106 (1998) [[arXiv:hep-ph/9709316](#)].
- [42] T. Hahn, Nucl. Phys. Proc. Suppl. 89, 231 (2000) [[arXiv:hep-ph/0005029](#)] and references therein.
- [43] A. Denner and T. Hahn, Nucl. Phys. B 525, 27 (1998) [[arXiv:hep-ph/9711302](#)].
- [44] K. m. Cheung, Phys. Rev. D 50, 4290 (1994) [[arXiv:hep-ph/9406228](#)].
- [45] K. Hagiwara, I. Watanabe and P. M. Zerwas, Phys. Lett. B 278, 187 (1992).